Injectable hyaluronic acid hydrogel loaded with BMSC and NGF for traumatic brain injury treatment

Luyu Wang [1], Dan Zhang [1], Yikun Ren, Shen Guo, Jinrui Li, Shanshan Ma, Minghao Yao [*], Fangxia Guan [**]

School of Life Science, Zhengzhou University, 100 Science Road, Zhengzhou, 450001, PR China

ARTICLE INFO

ABSTRACT

Injectable hydrogel has the advantage to fill the defective area and thereby shows promise as therapeutic implant or cell/drug delivery vehicle for tissue repair. In this study, an injectable hyaluronic acid hydrogel *in situ* dual-enzymatically cross-linked by galactose oxidase (GalOx) and horseradish peroxidase (HRP) was synthesized and optimized, and the therapeutic effect of this hydrogel encapsulated with bone mesenchymal stem cells (BMSC) and nerve growth factors (NGF) for traumatic brain injury (TBI) mice was investigated. Results from *in vitro* experiments showed that either tyramine-modified hyaluronic acid hydrogels (HT) or NGF loaded HT hydrogels (HT/NGF) possessed good biocompatibility. More importantly, the HT hydrogels loaded with BMSC and NGF could facilitate the survival and proliferation of endogenous neural cells probably by neurotrophic factors release and neuroinflammation regulation, and consequently improved the neurological function recovery and accelerated the repair process in a C57BL/6 TBI mice model. All these findings highlight that this injectable, BMSC and NGF-laden HT hydrogel has enormous potential for TBI and other tissue repair therapy.

1. Introduction

Traumatic brain injury (TBI) is a common neurotrauma and major cause of death and disability in the world. The external force can directly disrupt brain structure and function, leading to physical, cognitive, and behavioral symptoms and effects such as loss of consciousness, impairment of cognition and memory and other related neurological function. However, so far, there is no effective therapy in clinic [1]. Primary injury and secondary injury are two stages involved with the pathophysiological process of TBI [2]. Especially secondary injury causes cellular, chemical, tissue, or blood vessel changes in the brain that contribute to further destruction of brain tissue after initial impact, which leads to massive neuronal necrosis in the injured site, disrupts the blood-brain barrier and releases a large number of inflammatory factors, produces brain edema and neurological dysfunction [3,4]. The repair and rehabilitation of brain injury is a long-lasting challenging problem. Recently, many studies have presented that stem cell transplantation holds great promises for TBI treatment [5,6].

The development of stem cell therapy opens a new avenue for the brain function plasticity. When stem cells migrate to the damaged site of brain, they will survive and grow in a friendly microenvironment and crosstalk with cells and signals in many ways, including enhancing the secretion of neurotrophic factors, inhibiting neuroinflammation, promoting the synaptic formation of neurons at the injured site, and releasing neurotransmitters to promote the recovery of damaged nervous system [7]. Mesenchymal stem cells can also differentiate into neural cells at the lesion to replace the damaged or loss of neurons. Meanwhile, they can provide nutrition supplement, promote neurogenesis, protect the brain function, repair the injured brain structure and functional reconstruction [8–10]. Among them, bone marrow mesenchymal stem cells (BMSC) have attracted more attention due to their extensive sources, low immunogenicity and less ethical controversy [11]. However, stem cell retention, survival and differentiation in the lesion are far from satisfactory and hamper the brain functional recovery. Thus, an effective delivery of BMSC to the brain lesion and optimization of stem cell fate is still a technical challenge. It is known that building a suitable neural scaffold will be a pivotal strategy in favor of stem cell and drug delivery to the target area for cell-based therapy for TBI.

As the progress in tissue engineering field, development of new techniques will provide an innovation to solve the existing problems of stem cell transplantation. It was reported that improvement the therapeutic effect of stem cells has been achieved by tissue engineering modified methods in the treatment of a variety of diseases [12,13]. In TBI models, s series of hydrogels were developed as neural scaffolds by encapsulating stem cells and bioactive factors to repair cerebral function due to its three-dimensional network structure which is similar to neural tissue [14–16]. Among them, hyaluronic acid (HA) is a natural non-sulphated glycosaminoglycan, a major component of the extracellular matrix and gets involved in inflammatory response, angiogenesis and tissue regeneration [17,18]. HA has superior biocompatibility, biodegradability and easy to be chemically modified, which plays an important role in the process of wound healing [19,20]. A phenol-rich hyaluronic acid polymer has been of great interest for the development of *in situ* forming and injectable hydrogels enzymatically cross-linked by horseradish peroxidase (HRP) and galactose oxidase (GalOx) due to the controllable gelation rate, high specificity, and sensitive to outer condition changes.

Nerve growth factor (NGF) is a member of cytokine families that protects neuron survival, stimulates axonal growth and maintains synaptic plasticity, participates in physiological processes of neurotransmitter synthesis and release, and promotes the sensorimotor function recovery and axon regeneration [21–23]. However, the short half-life of exogenous NGF administration limits its bioactivity and therapeutic effect *in vivo*. Therefore, developing an efficient delivery of NGF with a hydrogel scaffold may better its bioactivity and provide a controlled-release of NGF, which is beneficial for repair and regeneration of neural injury [24–26]. By injection or spray-based minimal invasive approach, hydrogels enable remodeling in the lesion, encapsulate cells and/or biomolecules, and accurately fit to any irregular tissue defects [27,28].

Herein, we established a series of HT hydrogels dual-enzymatically cross-linked by GalOx and HRP. HT polymers performed as the natural neural scaffold material, BMSC as the seed cells, and NGF as the bioactive factor. The characterization and biocompatibility of HT hydrogels and HT/NGF hydrogels were investigated systematically. And the therapeutic effect of NFG and BMSC loaded in HT hydrogel was evaluated in TBI mice. All data suggested that this injectable HT hydrogel could successfully load of NFG and BMSC and has great potential for TBI treatment.

2. Experimental

2.1. Materials

Hyaluronic acid sodium salt (HA) from Streptococcus equi, horse radish peroxidase (HRP), tyramine hydrochloride, 2-(N-morpholino) ethanesulfonic acid (MES), 1-ethyl-3-(3-dimethylaminopropyl)-carbodiimide (EDC), N-hydroxysuccinimide (NHS), galactose oxidase (GalOx), and D-galactose were all purchased from Aladdin Chemical Reagent Co., Ltd. (Shanghai, China). The dialysis membrane (molecular cutoff = 3500 Da) was purchased from Solarbio Technology Co., Ltd. (Beijing, China). Murine bone marrow mesenchymal stem cells (BMSC) were purchased from Cell Bank of Chinese Academy of Sciences, Shanghai, China. Nerve growth factors (NGF) were from Staidson Biopharmaceuticals Co., Ltd. (Beijing, China). Calcein-AM/PI (Live/Dead kit) was obtained from Sigma Aldrich (St. Louis, MO, USA). CCK-8 kit was obtained from US Everbright, China. Alkaline phosphatase (ALP), glutamic-oxalacetic transaminase (GOT) and glutamic-pyruvic transaminase (GPT) assay kits were sourced from Solarbio Science &Technology Co., Ltd. (Beijing, China). All of the antibodies used in this study were purchased from Proteintech Group Inc. (Wuhan, China).

2.2. Synthesis of HT and HT/NGF hydrogels

HT hydrogels were prepared according to our previous method with some modifications [29]. The brief experimental steps are as follows: 0.5, 1, and 1.5 wt% HT polymers were dissolved in 100 mM/L D-galactose solution to obtain the pre-hydrogel solution, following by the addition of 1 U/mL HRP and 1 U/mL GalOx to synthesize HT hydrogel. For the preparation of HT/NGF hydrogels, 50, 100, 150, and 200 ng/mL NGF were added into the 0.5% pre-hydrogel solution respectively, following by addition of 1 U/mL HRP and 1 U/mL GalOx to induce gelation.

2.3. Characterization of HT hydrogels

An inverted tube test was used to determine the gelation time of 0.5, 1, and 1.5% HT hydrogels. When the GalOx and HRP were added to the solutions of HT polymers, the counting was started.

The injectable ability of HT hydrogels was first characterized by measuring the linear viscosity (η) under a frequency sweep mode (25 °C, 1–100 s^{-1}). Afterward, 500 μL of HT pre-hydrogel solution was transferred to a syringe to observe if it could be injected through a pinhole (25 G).

The water content of the HT hydrogels was calculated based on the formula: D (%) = [($W_w - W_d$)/W_w] × 100, where D denotes the water content of the hydrogels, W_w denotes the wet weight of the hydrogels, and W_d denotes the dried weight after freeze-drying.

The degradation performance of the hydrogels was investigated using the formula: L (%) = (W_t/W_i) × 100, where L denotes the mass residual rate after the hydrogels were immersed in PBS solution for 1, 3, 7, 14, 21, 28 and 35 days. The initial mass of hydrogels before immersing in PBS was labeled as W_i, and the mass of hydrogels after immersion for 1, 3, 7, 14, 21, 28 and 35 days was labeled as W_t.

The enzymatic degradation performance of the hydrogels was determined by another formula: L (%) = (W_t/W_i) × 100, where L denotes the mass residual rate after the hydrogels are immersed in 15 U/mL hyaluronidase solution hourly. The initial mass of the hydrogels before immersing in 15 U/mL hyaluronidase solution was labeled as W_i, and the mass of the hydrogels after immersion for each hour was labeled as W_t.

The swelling ratio (%) was calculated by the following equation: swelling ratio (%) = (W_s/W_i) × 100, where W_s is the weight of hydrogels immersed in PBS solution from day 1 to day 7, and W_i is the initial weight of the hydrogels. The measurement was repeated in triplicates.

The internal morphology of the HT hydrogel was characterized by scanning electron microscopy (SEM, FEI Quanta200, The Netherlands) after lyophilization, breakage and gold spraying.

The rheological behavior of the HT hydrogels was evaluated by a rheometer platform (TA DHR2, USA). The dynamic oscillation scanning angular frequency ranged from 0.1 to 100 rad/s, and the temperature and strain were set as 37 °C and 1%, respectively.

2.4. Cytocompatibility of HT and HT/NGF hydrogels

CCK-8 assay was used to assess the cytocompatibility of HT and HT/NGF hydrogels. The extracts from 0.5%, 1%, and 1.5% HT hydrogel and 0.5% HT hydrogels with different concentrations of NGF (50, 100, 150, and 200 ng/mL) were prepared by DMEM/F12 complete medium. The effect of different groups of HT and HT/NGF hydrogel extracts on the cell survival and proliferation of BMSC at the first day and second day was detected.

To evaluate the influence of hydrogels on the cellular activity, 3D culture was carried out as a test model. Briefly, BMSC were re-suspended with HT and HT/NGF pre-hydrogel solution at a density of 1 × 10^6 cells/mL, then HRP (1 U/mL) and GalOx (1 U/mL) were added to induce gelation. Each hydrogel (100 μL) was transferred to a 24-well plate, and 1 mL DMEM/F12 complete medium was added to each well and cultured at 37 °C in a cell incubator containing 95% air and 5% CO$_2$. After culturing for 3 and 5 days, the BMSC-loaded hydrogels were stained with Calcein-AM/PI working solution (Live/Dead kit) at 37 °C for 20 min, and

then observed under fluorescence microscopy (Leica DFC7000T, Germany). In addition, immunofluorescence of Ki67 was performed to analyze the proliferation of BMSC cultivated in hydrogels for 3 and 5 days, finally fluorescence was observed and photographed under inverted fluorescence microscope.

2.5. Animal experiments

2.5.1. Ethics statement

All animal procedures were performed in accordance with the Guidelines for Care and Use of Laboratory Animals of Zhengzhou University and approved by the Animal Ethics Committee of Zhengzhou University.

2.5.2. Blood compatibility and histocompatibility of HT hydrogel in vivo

The hemolysis rate was used to test the blood compatibility of HT hydrogels. First, HT hydrogels were prepared and soaked in normal saline for 30 min, then fresh mouse blood was collected and added. After further incubation for 1 h, hydrogels were removed and centrifuged at 2000 rpm for 5 min. Photographs were taken and the absorbance of supernatant was detected at 545 nm. The blood of mouse was put in deionized water as the positive control group. Normal saline instead of water was as the negative control group to calculate the hemolysis ratio. The hemolysis ratio was calculated by the following equation: hemolysis ratio (%) = $[(OD_T\text{-}OD_N)/(OD_P\text{-}OD_N)] \times 100$. OD_T, OD_N, and OD_P donate the absorbance value of test group (hydrogel group), negative group, and positive group, respectively. In addition, the morphology of red blood cells (RBCs) in NS, 0.5%HT hydrogel, 1%HT hydrogel, and 1.5%HT hydrogel groups were observed and captured by an inverted microscope.

Hematoxylin and eosin (HE) staining was performed to investigate the immune response of the implanted hydrogel scaffold. 100 μL 0.5% HT pre-hydrogel solution was subcutaneously injected at the dorsum of mice (3 injected points each mouse). The hydrogels and surrounding tissues were separated on day 3, 7, 14, and sectioned for HE staining to assess the biocompatibility of HT hydrogel in vivo. Moreover, the heart, liver, spleen, lung, kidney, and blood samples were harvest on day 14 for HE staining and biochemical analysis. ALP, GOT, and GPT were analyzed by the corresponding assay kits, with the normal mice set as control group.

2.5.3. Experimental groups and establishment of a moderate TBI model

C57BL/6 male mice (22–25 g) obtained from the Experimental Animal Center of Zhengzhou University were used in this study. BMSC were used as the seeded stem cells. TBI mice were divided into four groups randomly (6 mice in each group per batch): TBI mice treated with normal saline (NS) as the control group, three other groups of TBI mice were treated with NGF-loaded HT hydrogel scaffold (HT + NGF), BMSC-loaded HT hydrogel scaffold (HT + BMSC), and treated with BMSC and NGF-loaded HT hydrogel scaffold (HT + NGF + BMSC), respectively.

The TBI mice model was established by a typical Feeney's weight-drop method [30]. In brief, mice were given a normal preoperative hair removal under anesthesia. Then, the scalp was incised longitudinally along the median sagittal line, and the fascia was bluntly dissociated to expose the right skull. Next, a hole of diameter around 3 mm was opened which located at midway between the bregma and the lambda with the medial edge 1.5 mm lateral to the midline, and a craniocerebral percussion device (Shenzhen Ruiwode Lift Technology Co. Ltd, China) was adjusted so that the striker was hit precisely at the center of the opening. Subsequently, the striker was slowed down to make a contact with the dura, after a decline of 2 mm, free falling from a height of 20 cm with a 20 g impact hammer caused a moderate brain damage rapidly. Finally, routine cleaning of the wound and hemostasis were performed. After confirming that there was no active bleeding, the scalp was sutured. The mice's respiration and heartbeat were monitored, and the mice were kept warm until they completely woke up and their vital signs were stable.

2.5.4. HT hydrogel scaffold, NGF and BMSC injection

Seven days after TBI model establishment, C57BL/6 mice were anesthetized, and primary bone hole was exposed for in situ injection into the center of lesion. Briefly, the tip of microsyringe was placed 1.0 mm depth under the dura, and 20 μL pre-gel solution was slowly injected into the site of injury, which last approximately 2 min to reduce the leakage of cells along the needle tract. After injection, the needle was maintained in lesion for an additional 5 min before it was slowly pulled out. Finally, the scalp was sutured, and the mice were kept warm until they became active. Routine preventive antibiotics were applied, and the behavior tests such as limb movements, learning and memory ability, and wound healing of the TBI mice were observed at predetermined time points.

2.5.5. Neurological motor function assessment

On day 1, 3, 7, 14, 21, and 28 after treatment, the neurological motor function of the C57BL/6 mice (6 mice each group) was evaluated. The scores were determined by the double-blind method according to the modified neurological severity score (mNSS). The mNSS indexes including motor and sensory functions, balance, and reflexes were scored from 0 (healthy) to 18 (most severe) points in mice. The experimental protocols were described in our previous study [30].

2.5.6. Morris water maze

The learning and memory ability of the TBI C57BL/6 mice from day 23 to day 28 after treatment were investigated using a Morris water maze system (diameter 1.2 m, depth 0.6 m) with a platform (diameter 10 cm) located 2 cm underwater. The platform was marked with "○" so that mice could position themselves and search for the platform. Before entering the water, mice were placed on the platform for 10 s to acclimate themselves with the surrounding environment. Then, they were repositioned far away from the platform so that they were required to search for the marked platform. If the mice did not find the marked platform in 60 s, they would be placed again for an additional 10 s to refamiliarize themselves with the surrounding environment and underwent the test once more. The water temperature ranged from 19 °C to 21 °C, and entire test process was filmed with a camera. The escape latency and the time on the marked platform were recorded. On the last day, the platform was removed, mice were repositioned far away at the same place mentioned above, and swimming trails, the number of crossing platform, and the time that mice remained in the platform quadrant within 60 s were recorded.

2.5.7. Western blot

After treatment for 28 days, 6 mice in each group were sacrificed under anesthesia. Brain tissues around damaged areas were isolated and western blot were performed. In brief, tissues were lysed in lysis buffer. Then an equal amount of protein was loaded and separated by 10% sodium dodecyl sulfate-polyacrylamide gel electrophoresis gels and transferred to a polyvinylidene difluoride membrane (EMD Millipore, Billerica, MA, USA). After that, primary antibodies against neuronal differentiation related proteins (NSE, NeuN, and NFL, Proteintech), neurotrophic factors (BDNF, Proteintech), inflammation-associated protein (IL-6, Proteintech) and apoptosis-related proteins (Bax, Bcl-2, Proteintech) were incubated respectively, followed by horseradish peroxidase (HRP)-conjugated goat anti-rabbit IgG secondary antibody. β-actin was used as an internal control. The protein analysis was visualized by using Quantity One software (Azure Biosystems C300, Azure c300, USA).

2.5.8. Immunofluorescence staining

To evaluate the neural remodeling by the injected hydrogels, the proliferation and activity of neural cells in the hippocampus were examined using Ki67 and NeuN immunofluorescence staining. In addition, inflammatory response in lesion area were further examined by Arg1 and iNOS immunofluorescence staining.

2.5.9. Damaged area analysis

After 28 days of implantation, the brain tissues were preserved with 4% paraformaldehyde carefully. Frozen sections of the specimens were prepared to measure the volume of brain injury. Serial coronal sections were made at 2.0 mm before and after the lesion site, with the thickness of 20 μm for each brain slice. One section was randomly selected from each of 10 consecutive brain slices for HE staining. Image J software was used to analyze the lesion area of each group. The brain injury volume

formula is as follows: brain injury volume (unit: mm^3) = average injury area × the number of brain slices n × 10 × 2%. Then the brain tissues were photographed with a camera.

2.6. Statistical analysis

Data were given as means ± standard deviation (SD). Statistical analyses were plotted using Graph Pad Prism 8.0 software. One-way
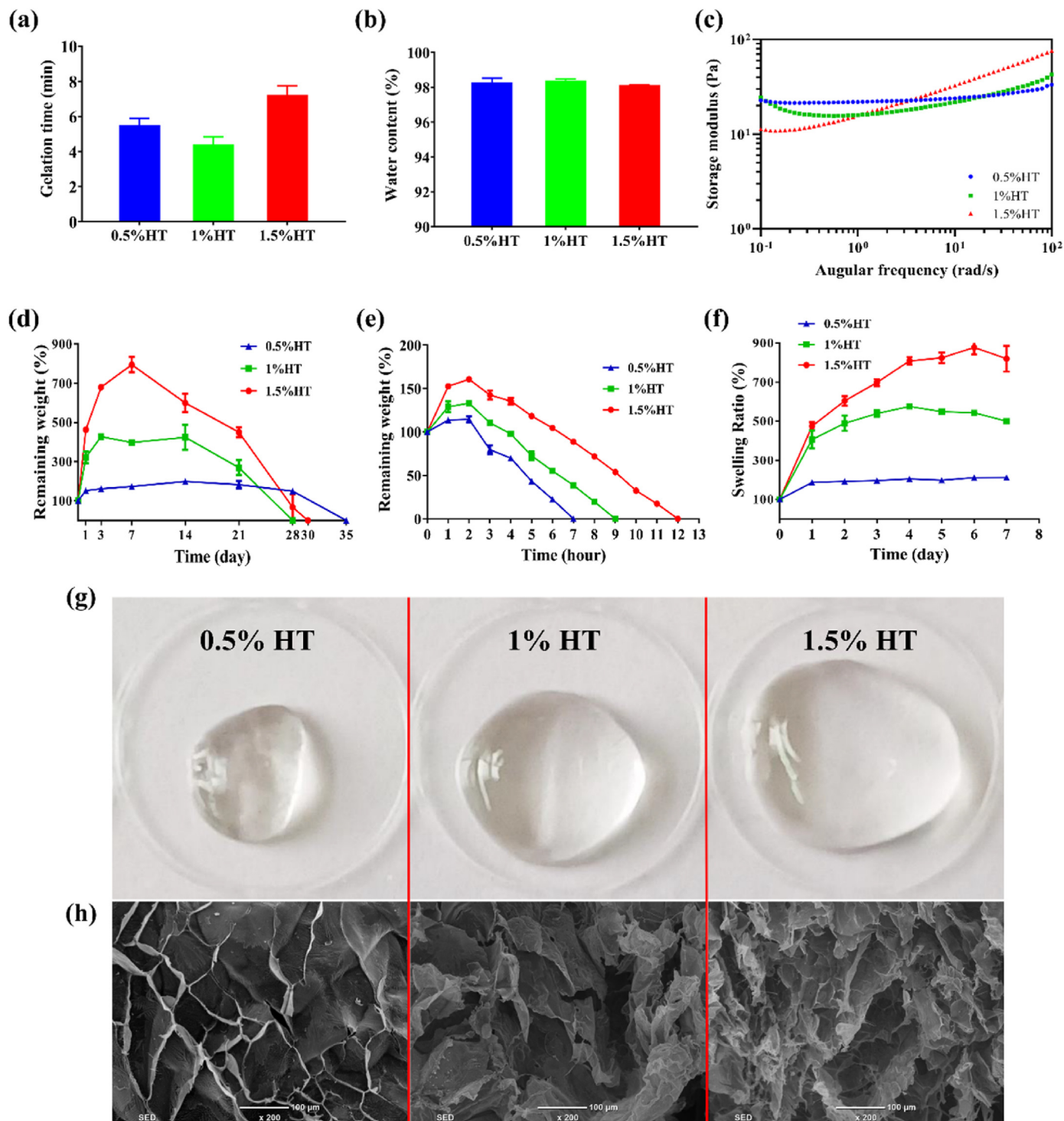

Fig. 1. Physical characterization of HT hydrogels. (a) Gelation time; (b) water content; (c) modulus of HT hydrogels measured by rheometer; (d) degradation rate of HT hydrogels in PBS; (e) degradation rate of HT hydrogels by 15 U/mL hyaluronidase; (f) swelling ratio of HT hydrogels; (g) photographs of HT hydrogel after soaking in PBS for 24 h; (h) internal microtopography of HT hydrogels by SEM. Scale bar represented 100 μm. Mean ± SD, n = 3.

ANOVA were performed to determine significance in statistical comparisons, $p < 0.05$ was considered statistically significant.

3. Results

3.1. Physical characterization of HT hydrogels

In our previous study, we developed a dual-enzymatically crosslinked HT hydrogel, and investigated the effect of enzyme activity on the physical and biological characteristics of HT hydrogels [29]. In this study, the influence of HT content on the physical and biological characteristis of HT hydrogels was further analyzed. The HT polymers of 0.5,

1, and 1.5 wt% were used to prepare hydrogels, and both of HRP and GalOx were set as 1 U/mL according to our previous study [29]. For the convenience of description, these hydrogels were named 0.5%HT, 1% HT, and 1.5%HT, respectively. The gelation time was 5.5 ± 0.7, 4.4 ± 0.8 and 7.2 ± 1.0 min respectively as shown in Fig. 1a, there was no linear correlation between gelation time and HT content. Injectable hydrogels have been widely studied due to their painless and minimally invasive merits. Hydrogels with shear-thinning ability can be injected directly into the desired position of injury, filling the wound well and making full contact with the wound site. Herein, a rheometer was applied to measure the relationship between HT hydrogel's viscosity and shear rate. As presented in Figure S1, increasing the shear rate reduced the viscosity,
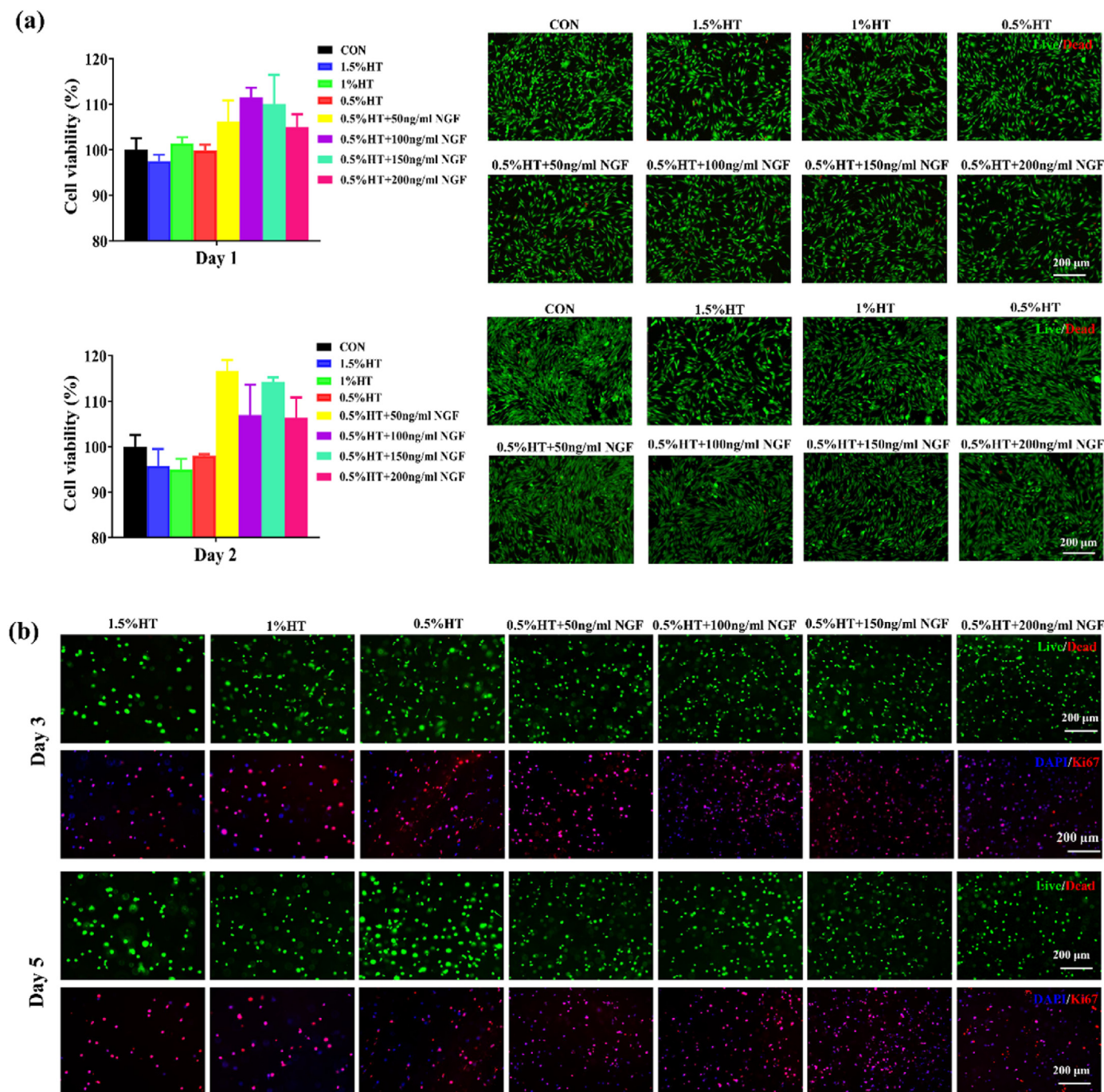

Fig. 2. Cytocompatibility and proliferation of BMSC by HT and HT/NGF hydrogels. (a) Cell viability of HT and HT/NGF hydrogel extracts for 1 and 2 days by CCK-8 assay; Calcein-AM/PI staining to detect cells morphology when cells were cultured with hydrogel extracts for 1 and 2 days; (b) Calcein-AM/PI fluorescence staining and Ki67 immunofluorescence staining of cells cultured within HT and HT/NGF hydrogels after 3 and 5 days. Scale bar represented 200 μm. Mean ± SD, n = 3.

demonstrating the well shear-thinning capacity of HT hydrogel. Besides, the insets in Fig. S1 showed that HT hydrogel could be easily injected and maintained its shape after injection without breaking, clogging, or dissolving, all confirming the excellent injectability of HT hydrogel. From Fig. 1b, all hydrogels possessed a water content about 98% (98.3 ± 0.4%, 98.4 ± 0.2% and 98.1 ± 0.1% for 0.5%HT, 1%HT, and 1.5%HT hydrogels). Rheological results from Fig. 1c showed that the storage moduli of 0.5%HT, 1%HT, 1.5%HT hydrogels were all less than 100 Pa similar to that of brain tissues and expected to be beneficial for neural differentiation [28]. The stability of hydrogels from Fig. 1d displayed that all hydrogels maintained in PBS solution for more than 28 days, and 0.5% HT hydrogel showed the highest stability. In addition, HT hydrogels could be biodegraded by hyaluronidase within 12 h. The completely degradation time of 0.5%HT, 1%HT and 1.5%HT hydrogels was 7 h, 9 h and 12 h, respectively (Fig. 1e). Hyaluronic acid is a super-absorbent and swelling material. The swelling ratio increased with the increase of HT content, and the maximum swelling ratios of 0.5%HT, 1%HT and 1.5% HT hydrogels were 211.4 ± 19.2%, 574.9 ± 18.2% and 857.3 ± 41.2%, respectively (Fig. 1f). The pictures of HT hydrogels after soaking in PBS solution for 24 h was presented in Fig. 1g, which was consistent with the result of swelling behavior. Additionally, the microstructure of HT hydrogels was also analyzed by SEM. Results from Fig. 1h showed that all hydrogel had a loose and porous structure, which is similar with natural extracellular matrix. In summary, the main difference of these hydrogels is the swelling ability. In order to minimize the risk of secondary damage during implantation, 0.5%HT hydrogel with low swelling ratio was selected as the scaffold for *in vivo* implantation.

3.2. Cytocompatibility of HT and HT/NGF hydrogels

The cytocompatibility of HT hydrogels and NGF-loaded hydrogels (named HT/NGF) was measured by CCK-8 assay. As shown in Fig. 2a, HT hydrogels decreased the viability of BMSC slightly on the first day and second day compared with control group (without hydrogel treatment). But the cell activity of BMSC in all hydrogel groups were greater than 95%, much more beyond the requirement of 70% as the international criteria [31]. And there was no significant difference among 0.5%HT, 1% HT, 1.5%HT hydrogel groups. Moreover, compared with the pure 0.5% HT hydrogel, NGF-loaded 0.5%HT hydrogels presented a better cell viability. The supplement of NGF could promote cell survival and growth, and the cell viability obviously improve the cell viability than control

group. Among these HT/NGF hydrogel groups, there was also no significant difference for cell viability. After CCK-8 assay, cells were labeled by Live/Dead kit (Calcein-AM/PI), almost all cells in each group were marked in bright green fluorescence (living cells) and cells' morphology in hydrogel groups presented no obvious change compared with control group, confirming the good cytocompatibility of HT and HT/NGF hydrogels.

Afterward, the cytocompatibility of these hydrogels was further analyzed by the three-dimensional cultivation method as shown in Fig. 2b. BMSC encapsulated in all hydrogels displayed well survival status (green fluorescence). Cell number of 1.5%HT hydrogel and 1%HT hydrogel was less than other hydrogel groups, which might be due to their higher swelling ratio and diluted cell density. Besides, there was nearly no difference among three hydrogel groups on day 3 and day 5. It was interesting that the encapsulated cells continuously leaked from hydrogels along with the process of cultivation and still maintained high viability as labeled with bright green (Fig. S2). This might partially explain why cell number within hydrogels did not increase as time goes on. Additionally, from the result of Ki67 immunofluorescence, cells cultured in hydrogels displayed a well proliferation behavior, indicating these hydrogels had little negative effect on cell growth. All these data from CCK-8 assay, Live/Dead fluorescence staining, and Ki67 immunofluorescence labeling demonstrate that these HT hydrogels and HT/NGF hydrogels possess good cytocompatibility *in vitro*.

Previous studies have indicated that the shear force exerted during injection has a negative effect on cell viability [32]. Here, the Live/Dead fluorescence staining of BMSC before and after injection was carried out to observe the influence of shear force. Results in Fig. S3 demonstrated that the shear force during the injection did not obviously affect cell viability in our study. The possible reason was that the gelation time of 0.5%HT hydrogel is 5.5 min, and the injection process could finish before gelation. During the injection, shear force of pre-hydrogel solution is far less than that of hydrogel. Therefore, the produced shear force during injection of HT pre-hydrogel is very mild, and the caused negative effect on cell viability could be negligible.

3.3. Blood compatibility and histocompatibility of HT hydrogel

3.3.1. In vitro hemolysis test for blood compatibility

As shown in Fig. 3a, results of hemolysis test showed that there was nearly no hemolysis reaction in HT hydrogel groups. The hemolysis rates
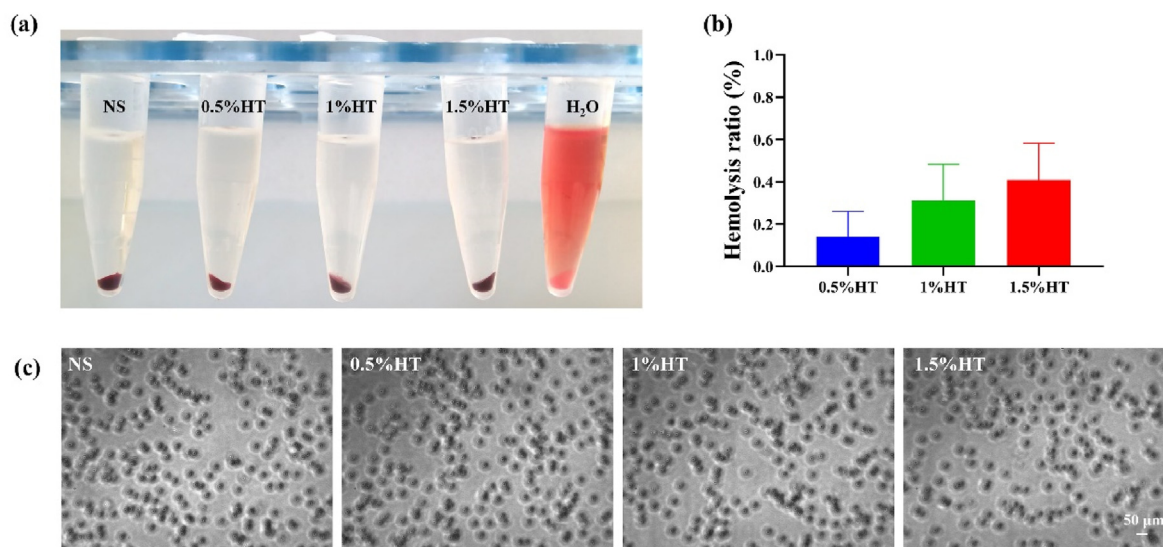

Fig. 3. Hemolysis test *in vitro* for evaluation of blood compatibility of HT hydrogels. (a) Images of RBCs treated with normal saline (NS), 0.5%HT, 1%HT, 1.5%HT and H₂O. H₂O group and NS group were positive control and negative control group, respectively; (b) hemolysis ratio of 0.5%HT, 1%HT and 1.5%HT hydrogels; (c) Images of RBCs in NS, 0.5%HT hydrogel, 1%HT hydrogel, and 1.5%HT hydrogel groups. Mean ± SD, n = 3.
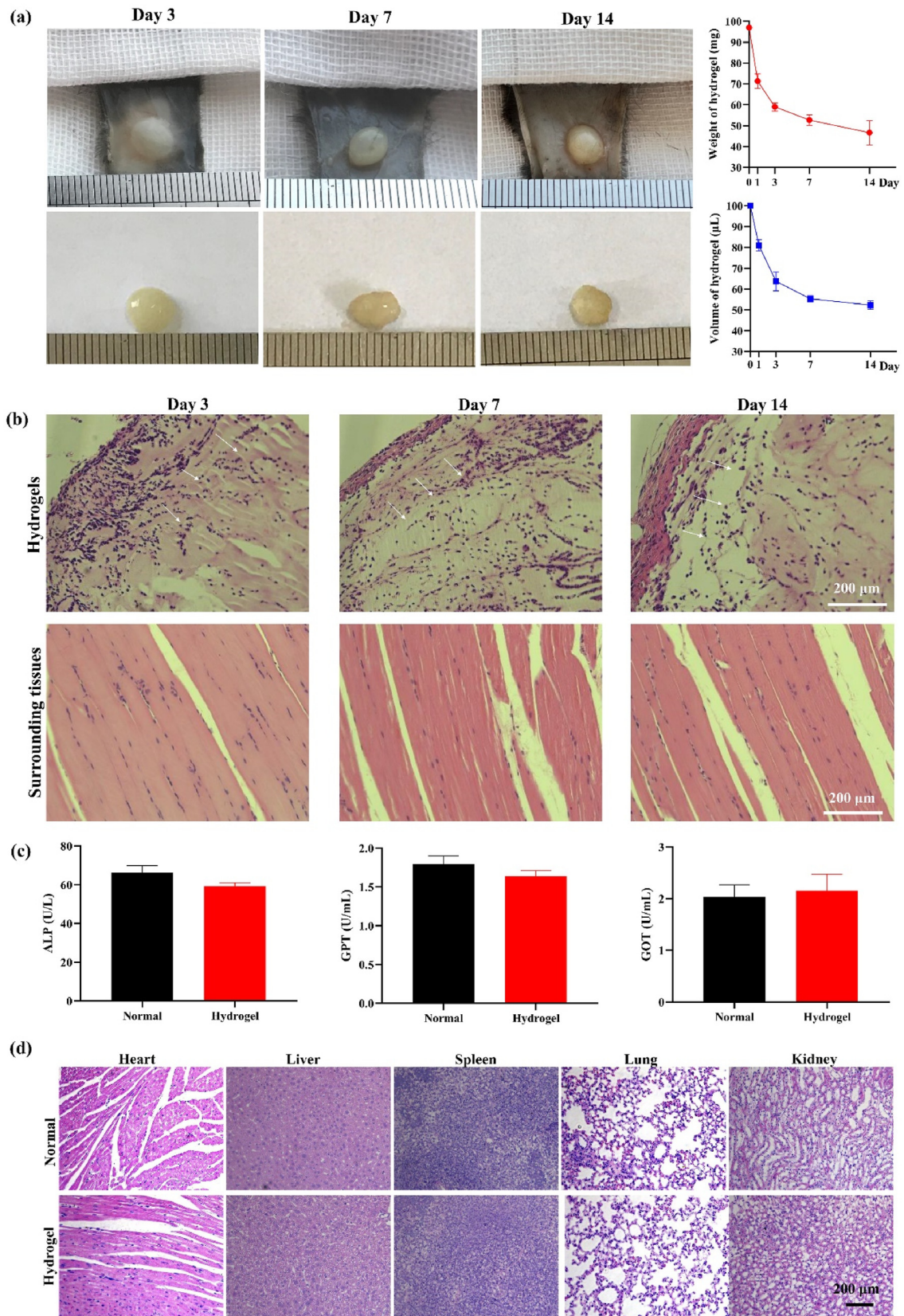
Fig. 4. *In situ* subcutaneous implantation for assessment of histocompatibility of 0.5%HT hydrogel. (a) Pictures of 0.5%HT hydrogel after 3, 7 and 14 days of subcutaneous injection; statistical results of the weight and volume of hydrogels after 1, 3, 7 and 14 days of subcutaneous injection; (b) HE staining of subcutaneously extracted hydrogels (the white arrows were inflammatory cells); HE staining of tissues around the subcutaneous implantation site; (c) blood biochemistry test of the normal mice (Normal group) and HT hydrogel-implanted mice (Hydrogel group) on day 14, ALP: alkaline phosphatase, GPT: glutamic-pyruvic transaminase, GOT: glutamic-oxalacetic transaminase; (d) HE staining of main organs in Normal group and Hydrogel group on day 14. Scale bar represented 200 μm. Mean ± SD, n = 3.

of 0.5%HT, 1%HT and 1.5%HT hydrogels were 0.14 ± 0.07%, 0.31 ± 0.20%, and 0.41 ± 0.20%, respectively (Fig. 3b). The data fully meet the demands of the international standard of biomaterials hemolysis rate 5%, indicating that these hydrogels have good blood compatibility [33]. Besides, the morphology of RBCs (red blood cells) after treated with hydrogels was observed using a microscope. All treated RBCs maintained a biconcave disc shape, similar to the shape of healthy RBCs in NS group from Fig. 3c.

3.3.2. Histocompatibility assessment

100 μL of 0.5%HT hydrogel was subcutaneously injected at the dorsum of C57BL/6 mice to evaluate the histocompatibility. The experimental mice had normal eating and activity, and there was no bleeding and swelling after subcutaneous implantation. Weight and volume of hydrogels were gradually down, indicating these hydrogels are biodegradable *in vivo* (Fig. 4a). As shown in Fig. 4b, lots of cells infiltrated into hydrogels, which contained inflammatory cells (white arrow), however, most cell infiltration occurred in the marginal area of hydrogels, and there was almost no inflammatory response in the tissues around subcutaneous injection site, suggesting that HT hydrogel has good histocompatibility and could be further applied *in vivo*.

In order to further evaluate the systemic biosafety of 0.5%HT hydrogel, the biochemical analysis of blood and HE staining of main organs on day 14 were also performed. From Fig. 4c, the blood biochemical indexes of ALP (alkaline phosphatase), GPT (glutamic-pyruvic transaminase), and GOT (glutamic-oxalacetic transaminase) displayed no significance between the healthy mice and 0.5%HT hydrogel-implanted mice. As presented in Fig. 4d, there was no obvious pathological change between Normal group and Hydrogel group, indicating that the implantation of 0.5%HT hydrogel would not cause noticeable impair to vital organs and tissues. All these above results highlighted the excellent biocompatibility of 0.5%HT hydrogel *in vivo*.

3.4. In vivo testing

To further investigate *in vivo* neural repair efficacy of HT hydrogel combined with BMSC and NGF. The moderate traumatic brain injury (TBI) contusion model of C57BL/6 mice was performed according to our previous method [34]. Treatment was performed 7 days after the establishment of TBI model. The timeline of animal experiment was as follows (Scheme 1): the day of hydrogel implantation was set as day 0; modified neurological severity score (mNSS) was performed on 1, 3, 7, 14, 21, and 28 days after implantation; Morris water maze (MWM) test was performed from day 23–28; and brain tissues were collected to measure the damaged volume, western blot and immunofluorescence assays on the 28th day.

3.4.1. BMSC and NGF-loaded HT hydrogel implantation promotes the recovery of neuromotor function in TBI mice

From Fig. 5, the mNSS score of TBI mice in HT + NGF group, HT + BMSC group and HT + NGF + BMSC group were significantly decreased compared with NS group (p < 0.05) on the 14th day after implantation. With the prolongation of treatment time, mNSS score in the HT + BMSC
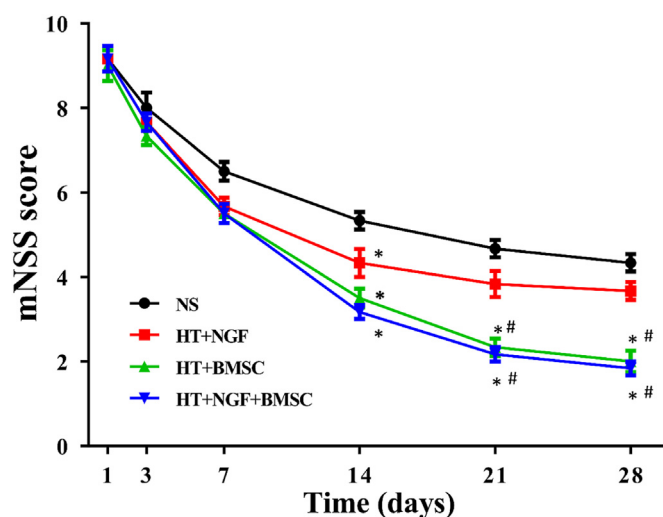
Fig. 5. The mNSS score of implanted TBI mice in each group, which revealed the recovery of motor ability from day 1 to day 28 (*p < 0.05 compared with NS, #p < 0.05 compared with HT + NGF hydrogel, mean ± SD, n = 6).

group and HT + NGF + BMSC group continued to reduce significantly on the 21st and 28th days after implantation compared with not only NS group (p < 0.05) but also HT + NGF group (p < 0.05). These results indicated that in the early stage of implantation, the HT + NGF, HT + BMSC and HT + NGF + BMSC groups had good therapeutic effect and could promote the recovery of neuromotor function. In the meantime, the outcome of TBI mice treated by HT + BMSC hydrogel and HT + NGF + BMSC hydrogel implantation was better than HT + NGF hydrogel implantation on day 21 and day 28.

3.4.2. BMSC and NGF-loaded HT hydrogel implantation improves the recovery of learning and memory function in TBI mice

To evaluate the recovery of learning and memory abilities of TBI mice in each group, Morris Water Maze (MWM) behavior test was performed from day 23 to day 28 after treatment. The results were presented in Fig. 6. As shown in Fig. 6b, the escape latency in HT + BMSC group and HT + NGF + BMSC group was significantly lower than that in NS group (p < 0.05), indicating that mice in HT + BMSC group and HT + NGF + BMSC group could better adapt to the training environment. As shown in Fig. 6a, c and 6d, compared with NS group and HT + NGF group, mice in HT + BMSC group and HT + NGF + BMSC group crossed the platform more frequently, and mice in HT + NGF + BMSC group stayed longer in the target quadrant (p < 0.05). Moreover, in comparison to the HT + BMSC group, HT + NGF + BMSC group demonstrated a better outcome. These results indicated that HT/BMSC hydrogel and HT/NGF/BMSC hydrogel had better therapeutic effect and improved the recovery of learning and memory function of TBI mice, and HT/NGF/BMSC hydrogel treatment performed the best.
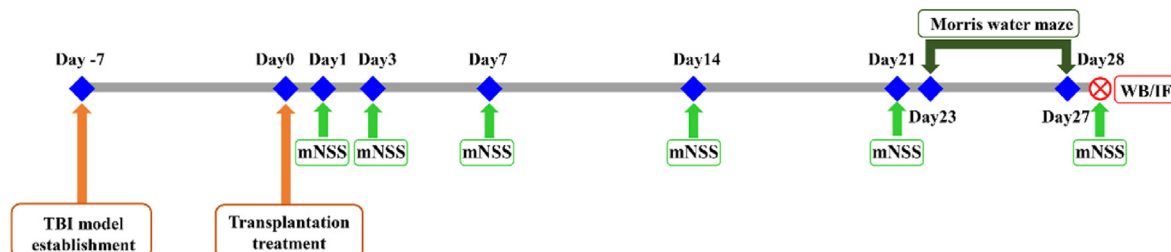
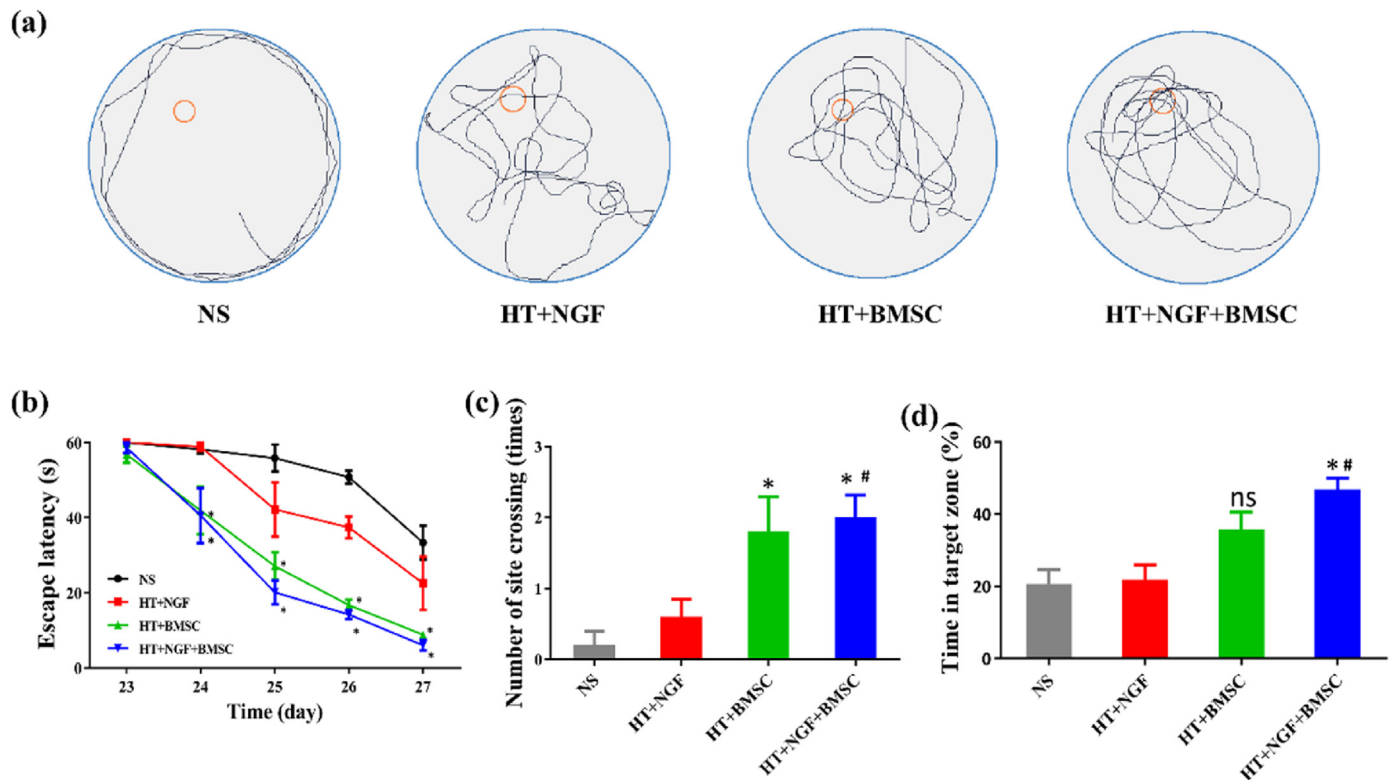**Scheme 1.** Timeline and procedures of *in vivo* experiments.

Fig. 6. MWM experiment results of mice in each group after implantation (a) Swimming trails; (b) escape latency; (c) number of platform crossing; (d) time in the target zone (*p < 0.05 compared with NS group, #p < 0.05 compared with HT + NGF group, mean ± SD, n = 6).

3.4.3. BMSC and NGF-loaded HT hydrogel implantation alleviates the inflammatory response and apoptosis in the injured site of TBI mice

After 28 days transplantation, the expression of inflammation-related protein (IL-6) and apoptosis-related proteins (Bax and Bcl-2) was detected by western blot to elucidate the curative effect of BMSC and NGF-loaded HT hydrogel on brain injury repair. As shown in Fig. 7a and b, the expression of inflammatory related protein IL-6 in HT + NGF + BMSC group was decreased significantly compared with that of NS group (p < 0.05), indicating that the inflammatory response after transplantation was reduced in TBI mice. Compared with NS group, the expression of apoptotic factor Bax decreased in all treatment groups, while its expression was significantly decreased only in HT + BMSC and HT + NGF + BMSC groups (p < 0.05). Although the expression of anti-apoptotic factor Bcl-2 increased in all treatment groups, only HT + NGF + BMSC group was significantly increased compared with NS group (p < 0.05). The enhanced expression of proapoptotic protein Bax and low expression of apoptotic inhibitory protein Bcl-2 both indicated that hydrogel implantation could obviously inhibit the neuronal apoptosis. As shown in Fig. 7c, compared with the NS group, stronger immunofluorescence intensity of Arg1 (marker of M2 macrophage/microglia) and weaker immunofluorescence intensity of iNOS (marker of M1 macrophage/microglia) were observed in HT + NGF, HT + BMSC, and the HT + NGF + BMSC groups, suggesting that hydrogel treatments could promote the polarization of macrophage/microglia from M1 type to M2 type. In a word, the above results of western bolt and immunofluorescence manifested that BMSC and NGF-loaded HT hydrogel implantations could significantly mitigate TBI-induced neuroinflammation and apoptosis around the injured site of TBI mice.

3.4.4. BMSC and NGF-loaded HT hydrogel injection enhances the cell survival of neurons in the injured site and neurogenesis of TBI mice

The expressions of brain-derived neurotrophic factor (BDNF) and neuron-specific markers (NFL, NSE and NeuN) in the damaged tissues were detected by western bolt to elucidate the curative effect of BMSC and NGF-loaded HT hydrogel on brain injury repair after 28 days of treatment. From Fig. 8a and b, in contrast with NS group, the expression of BDNF was increased in all hydrogel treatment groups, and significantly increased in the HT + NGF + BMSC group (p < 0.05). Similarly, the expression of NFL was increased in all hydrogel treated groups, and significantly increased in HT + BMSC and HT + NGF + BMSC groups compared with NS group (p < 0.05). The expression of NSE in HT + BMSC and HT + NGF + BMSC groups was increased significantly compared with NS and HT + NGF groups (p < 0.05). In addition, the expression of NeuN was promoted in all treatment groups compared with NS group (p < 0.05). These results suggest that HT + BMSC and HT + NGF + BMSC groups produce more neurotrophic cytokines and neuron-related proteins, which effectively promote the neural repair and functional recovery in TBI mice. Furthermore, the proliferation of neural cells in the hippocampus was detected by immunofluorescence staining (Fig. 8c). Compared with NS group, the positive expression of both Ki67 and NeuN in DG region was obviously increased in the HT + BMSC and HT + NGF + BMSC groups, and the positive expression in HT + NGF + BMSC group was the most abundant, which indicated that there were more proliferative cells in DG region and enhanced therapeutic effect by BMSC and NGF-loaded HT hydrogel treatment.

3.4.5. BMSC and NGF-loaded HT hydrogel accelerates the healing process of damaged tissue in TBI mice

After 28 days of *in situ* injection, the damaged tissue volume in each group was observed by HE staining (Fig. 9a), gross morphology (Fig. 9c), and then quantitatively analyzed by Image J (Fig. 9b). Compared with NS group, the damaged volume in the treatment groups (HT + NGF group, HT + BMSC group and HT + NGF + BMSC group) were all decreased significantly (p < 0.05). Compared with the HT + NGF group, the damaged area of HT + BMSC and HT + NGF + BMSC groups were smaller and the therapeutic effect were more obvious (p < 0.05).
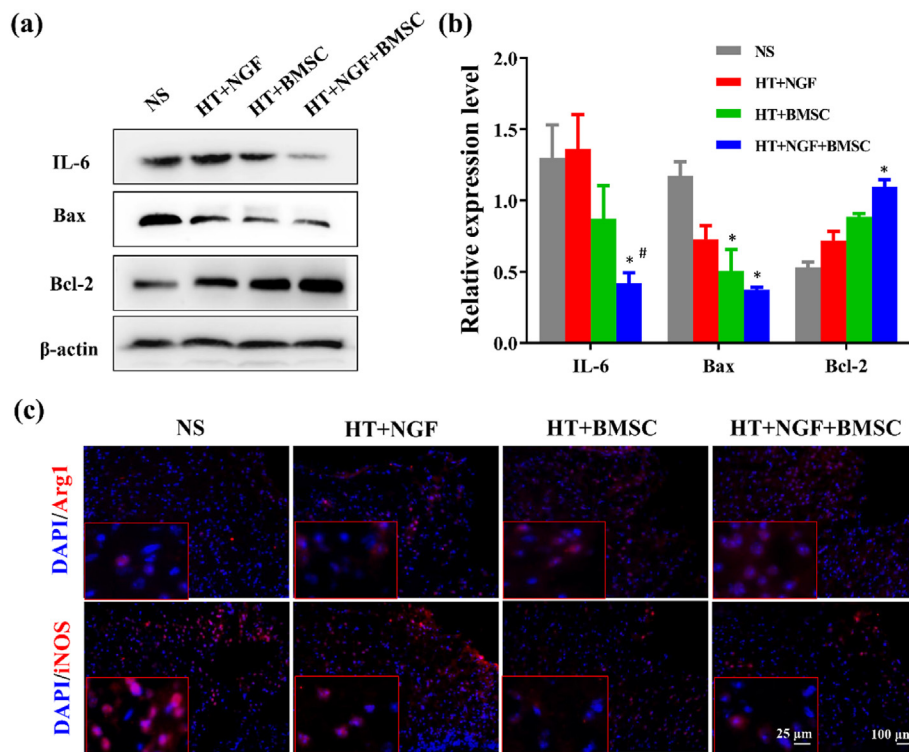
(a)

(b)

(c)

Fig. 7. Expression of inflammation and apoptosis-related proteins in the damaged brain tissues of each group after 28 days' treatment. (a) Western blot images of IL-6, Bax and Bcl-2; (b) quantitative analysis of western blot results of IL-6, Bax and Bcl-2; (c) immunofluorescence staining of Arg1 and iNOS, DAPI labeled the nucleus, scale bar represented 25 and 100 μm. β-actin was used as a protein loading control; *p < 0.05 compared with NS group, #p < 0.05 compared with the HT + NGF group; mean ± SD, n = 3.

Particularly, the lesion volume in HT + NGF + BMSC group was the lowest among all the treatment groups, highlighting the best recovery outcome of the combined treatment (HT + NGF + BMSC hydrogel).

4. Discussion

TBI is a serious neurotrauma disease with a high incidence of death and disability globally, which causes a sudden serious brain structure disruption, large number of neuronal death and long-lasting or irreversible neurological dysfunction [35,36]. Currently, the effect of clinical treatment on neurological function after TBI is far from satisfaction [37]. At present, more and more preclinical studies or clinical trial by using mesenchymal stem cells (MSCs), induced pluripotent stem cells (iPSCs) and neural stem cells (NSCs) have been performed to evaluate the safety and efficacy of stem cell therapy for TBI [38]. Stem cell therapy has brought a new era for some intractable diseases include TBI. Stem cells transplantation could promote neural regeneration and functional reconstruction through multiple mechanisms including inhibition of neuroinflammation, direction of neural differentiation, secretion of neurotrophic factors and so on [39,40]. However, stem cell-based therapy still faces many technical bottlenecks, such as a low retention and survival of stem cells in the injured niche after transplantation, inefficient neural differentiation, which limit its therapeutic effects. To solve these problems, encapsulation of stem cells with hydrogel material to prompt cell retention and survival is an alternative promising and effective strategy.

A neural scaffold should possess a series of essential characteristics for supporting transplanted cell growth and simultaneously matching the brain microenvironment. Hydrogel is one of the widely studied tissue engineering material, also an excellent carrier for stem cells, bioactive factors and drugs. An ideal hydrogel includes a controllable gelation process, high water content, porosity, appropriate rheological behavior, suitable degradation performance, injectability, and the most important property of well biocompatibility. Currently, a variety of hydrogel materials have been studied in nervous system diseases, such as hyaluronic

acid, sodium alginate, gelatin, collagen and polypeptides [14,41–44]. As a major component of extracellular matrix of neural cells, hyaluronic acid plays an important role in maintaining the brain homeostasis by affecting cell migration, proliferation, differentiation and other cellular behaviors [18,45,46]. Hyaluronic acid hydrogels have good biocompatibility and have been widely used in tissue engineering and regenerative medicine. Nerve growth factor (NGF) regulates the production of neurotransmitters and improves the survival, growth and differentiation of neurons, and has shown superior ability to repair nerve injuries in animal models [47, 48].

In this study, we synthesized and optimized an injectable hyaluronic acid hydrogel (HT hydrogel) through *in situ* enzymatically crosslinked technique by HRP and GalOx, and used it as a neural scaffold to deliver BMSC and NGF for TBI treatment. The 0.5%HT hydrogel possessed sufficient moisture (about 98%), low swelling ratio and appropriate rheological behavior that meet the physiological requirements for brain tissue repair and reduce the frictional irritation to the surrounding tissue [49, 50]. A gelation time of 5 min would benefit the injection process, because a longer time of operation will lead to the loss of loaded cell and NGF. The continuous and porous structure facilitates the permeation of nutrients, exchange of oxygen and carbon dioxide, and discharge of metabolites, which could provide a friendly environment for cell survival, extension and proliferation. The superior cytocompatibility of the 0.5%HT and 0.5%HT/NGF hydrogels confirmed by 3D culture model and Ki67 immunofluorescence staining could ensure the survival and proliferation of loaded BMSC. Good biocompatibility of this hydrogel verified by hemolysis test, blood biochemistry assays, and HE staining is a prerequisite of its further application *in vivo*.

For animal treatment, normal saline (NS), HT + NGF, HT + BMSC and HT + NGF + BMSC hydrogels were micro-injected into the core of the lesion on day 7 after the establishment of TBI model. One week after TBI, the harsh microenvironment of lesion dramatically alleviated, and the severe inflammatory response basically subsided, which provide a relative stable living microenvironment for the implanted cells [51]. Therefore, the timepoint (7 days after TBI model) was chosen for
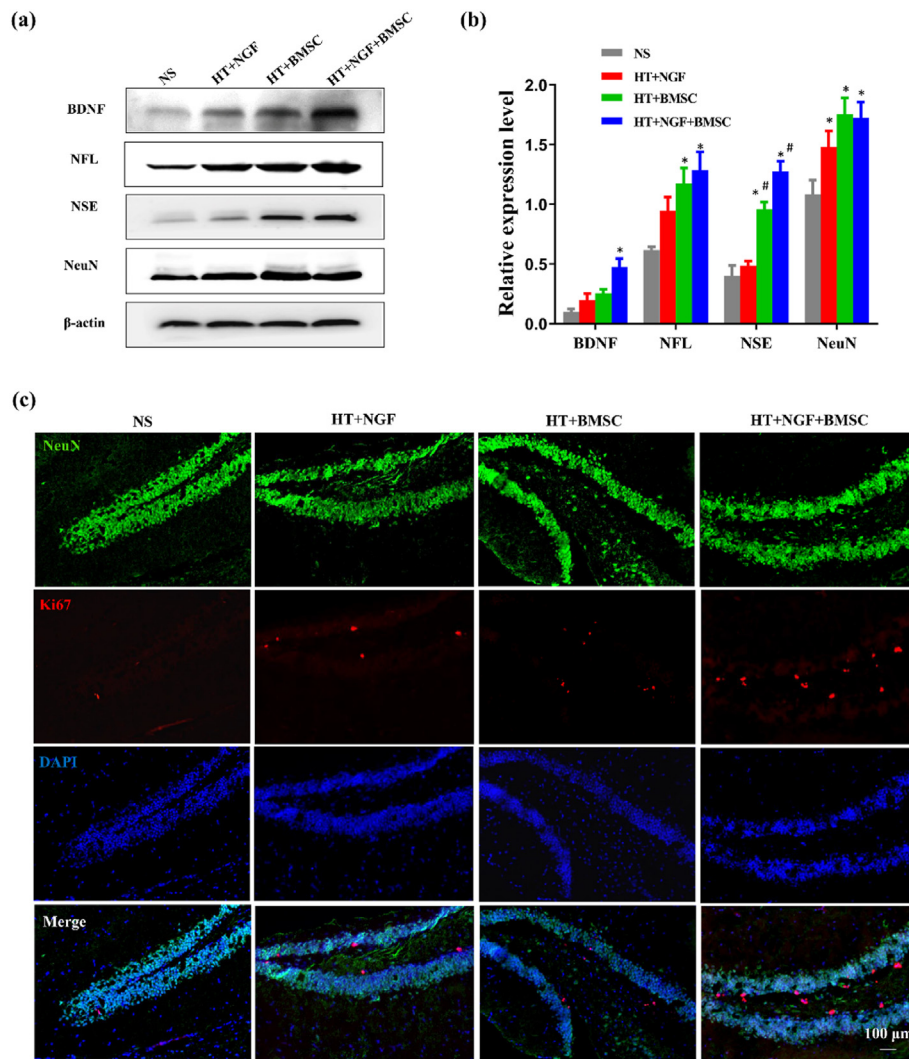
Fig. 8. Expression of neuro-related proteins in the damaged brain tissue and DG region of each group after 28 days' treatment. (a) Western blot of BDNF, NFL, NSE and NeuN; (b) quantitative analysis of western blot results of BDNF, NFL, NSE and NeuN; (c) immunofluorescence staining of Ki67 and NeuN to detect the neural cell proliferation in DG region after 28 days' treatment, DAPI label the nucleus, scale bar represented 100 μm. β-actin was used as internal control; *p < 0.05 compared with NS group, #p < 0.05 compared with HT + NGF group; mean ± SD, n = 3.
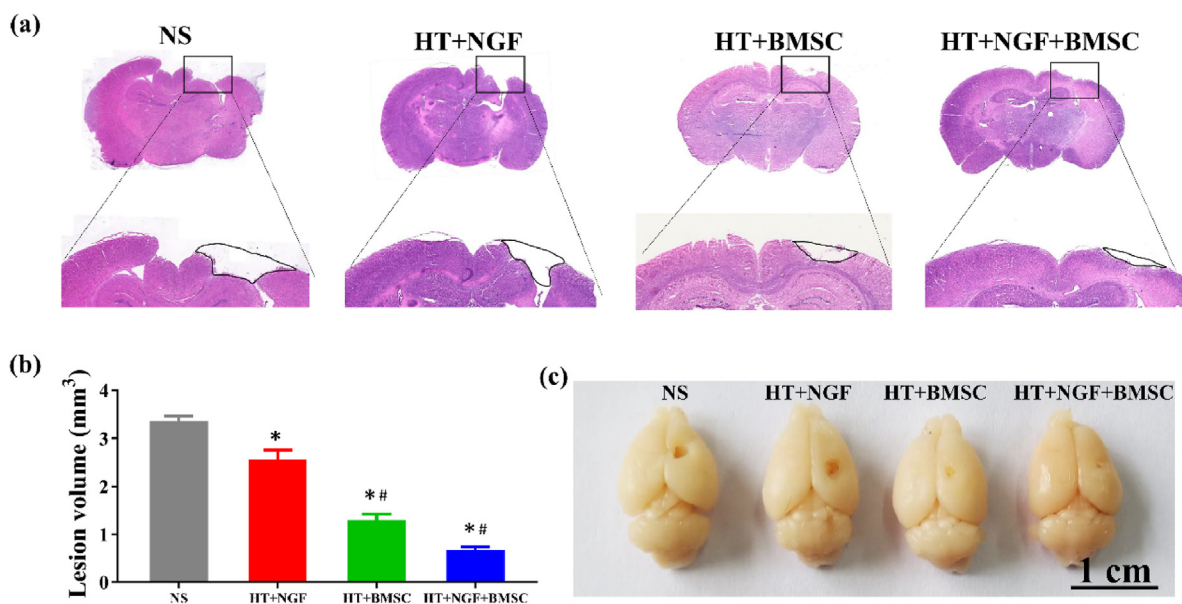

Fig. 9. Statistical results of brain tissue defect area in each group after 28 days' transplantation. (a) HE staining of tissue sections; (b) quantitative analysis of lesion volume, and (c) representative photographs of the damaged volume in each group after 28 days' treatment. *p < 0.05 compared with NS group, #p < 0.05 compared with HT + NGF group, mean ± SD, n = 3.

treatment. In addition, after 7 days, a cavity formed at the injury site, providing space for *in situ* hydrogel injection [52–54]. The mNSS scoring and MWM are very common tests to assess the neurological function situation including motor function, learning and memory ability [55,56]. The results of mNSS indicated that all the three treatment groups had improved neural function in TBI mice, and HT + BMSC and HT + NGF + BMSC groups exhibited better therapeutic recovery of neuromotor function. The results of MWM demonstrated that the number of crossing platform and staying time in target zone significantly increased in HT + BMSC and HT + NGF + BMSC groups compared with others. The motor function and cognition showed a consistent rising trend. Therefore, both mNSS and MWM test results confirmed that HT + BMSC and HT + NGF + BMSC groups indeed promoted the neurological function recovery in TBI mice after treating for 28 days, when compared with NS group.

In addition, we further analyzed more related protein expressions for cell growth including IL-6, Bax, Bcl-2, BDNF, NFL, NSE, NeuN by western blot. Combined with immunofluorescence staining of Arg1, iNOS, NeuN and Ki67, these data suggested that HT + BMSC and HT + NGF + BMSC groups markedly reduced neuroinflammation, inhibited cell apoptosis, promoted neurotrophic factor secretion, and enhanced endogenous neural cell survival and proliferation. Moreover, data analysis of the damaged volume indicated that composite hydrogels significantly facilitated the repair process of brain damage. Therefore, it is clear that BMSC and NGF-loaded HT hydrogel makes a striking contribution to the neurological function recovery and tissue regeneration in TBI mice, and the working mechanism includes apoptosis inhibition, immunoregulation, neurotrophic factors secretion and neurogenesis synergistically.

5. Conclusions

In this work, dual-enzymatically cross-linked hyaluronic acid hydrogels by GalOx and HRP were developed as a novel neural scaffold to simultaneously load NGF and BMSC for TBI treatment. HT hydrogels have good injectability, stability, biodegradability, low storage modulus (<100 Pa), and superior biocompatibility. 0.5%HT hydrogel with the lowest swelling ratio was more suitable as the implanted scaffold compare with 1%HT and 1.5%HT hydrogel. *In situ* injection of NGF and BMSC-loaded HT hydrogel could significantly promote the functional recovery of motor, learning and memory ability, and accelerate the healing process of damaged brain tissues. The molecular mechanism mainly involves that hydrogel implantation not only provides a positive nutrition supply for cell survival and proliferation, but also suppresses neuroinflammation and apoptosis. These findings provide a solid basis for the application of BMSC and NGF loaded HT hydrogel in TBI treatment.

Credit author statement

Luyu Wang: Resources, Methodology, Data curation, Writing – original draft. Dan Zhang: Resources, Methodology, Writing – review & editing. Yikun Ren: Methodology, Writing – review & editing. Shen Guo: Methodology. Jinrui Li: Resources. Shanshan Ma: Writing – review & editing. Minghao Yao: Conceptualization, Supervision, Validation, Writing – review & editing. Fangxia Guan: Conceptualization, Investigation, Writing – review & editing.

Declaration of competing interest

The authors declare no competing financial interest.

Acknowledgments

Appendix A. Supplementary data

Supplementary data to this article can be found online at https://doi.org/10.1016/j.mtbio.2021.100201.

References

[1] M.G. Maggio, R. De Luca, F. Molonia, B. Porcari, M. Destro, C. Casella, R. Salvati, P. Bramanti, R.S. Calabro, Cognitive rehabilitation in patients with traumatic brain injury: a narrative review on the emerging use of virtual reality, J. Clin. Neurosci. 61 (2019) 1–4.

[2] M.A. Panaro, T. Benameur, C. Porro, Extracellular vesicles miRNA cargo for microglia polarization in traumatic brain injury, Biomolecules 10 (6) (2020), 901.

[3] J. Feng, J. Jiang, Traumatic brain injury in 2019: databases, biomarkers, and stratified treatment, Lancet Neurol. 19 (1) (2020) 5–7.

[4] B. Solomon, R.J. Young, D. Rischin, Head and neck squamous cell carcinoma: genomics and emerging biomarkers for immunomodulatory cancer treatments, Semin. Cancer Biol. 52 (Pt 2) (2018) 228–240.

[5] A. Dekmak, S. Mantash, A. Shaito, A. Toutonji, N. Ramadan, H. Ghazale, N. Kassem, H. Darwish, K. Zibara, Stem cells and combination therapy for the treatment of traumatic brain injury, Behav. Brain Res. 340 (2018) 49–62.

[6] M. Carbonara, F. Fossi, T. Zoerle, F. Ortolano, F. Moro, F. Pischiutta, E.R. Zanier, N. Stocchetti, Neuroprotection in traumatic brain injury: mesenchymal stromal cells can potentially overcome some limitations of previous clinical trials, Front. Neurol. 9 (2018), 885.

[7] T. Yasuhara, S. Kawauchi, K. Kin, J. Morimoto, M. Kameda, T. Sasaki, B. Bonsack, C. Kingsbury, N. Tajiri, C.V. Borlongan, I. Date, Cell therapy for central nervous system disorders: current obstacles to progress, CNS Neurosci. Ther. 26 (6) (2020) 595–602.

[8] J. Chen, S. Ren, D. Duscher, Y. Kang, Y. Liu, C. Wang, M. Yuan, G. Guo, H. Xiong, P. Zhan, Y. Wang, H.G. Machens, Z. Chen, Exosomes from human adipose-derived stem cells promote sciatic nerve regeneration via optimizing Schwann cell function, J. Cell. Physiol. 234 (12) (2019) 23097–23110.

[9] Y. Wang, J. Pan, D. Wang, J. Liu, The use of stem cells in neural regeneration: a review of current opinion, Curr. Stem Cell Res. Ther. 13 (7) (2018) 608–617.

[10] F. Cofano, M. Boido, M. Monticelli, F. Zenga, A. Ducati, A. Vercelli, D. Garbossa, Mesenchymal stem cells for spinal cord injury: current options, limitations, and future of cell therapy, Int. J. Mol. Sci. 20 (11) (2019), 2698.

[11] M. Das, K. Mayilsamy, S.S. Mohapatra, S. Mohapatra, Mesenchymal stem cell therapy for the treatment of traumatic brain injury: progress and prospects, Rev. Neurosci. 30 (8) (2019) 839–855.

[12] G. Shojaati, I. Khandaker, K. Sylakowski, M.L. Funderburgh, Y. Du, J.L. Funderburgh, Compressed collagen enhances stem cell therapy for corneal scarring, Stem Cells Transl. Med. 7 (6) (2018) 487–494.

[13] H. Li, A.Q. Ye, M. Su, Application of stem cells and advanced materials in nerve tissue regeneration, Stem Cell. Int. 2018 (2018), 4243102.

[14] M. Yao, F. Gao, R. Xu, J. Zhang, Y. Chen, F. Guan, A dual-enzymatically cross-linked injectable gelatin hydrogel loaded with BMSC improves neurological function recovery of traumatic brain injury in rats, Biomater. Sci. 7 (10) (2019) 4088–4098.

[15] Y. Wu, J. Wang, Y. Shi, H. Pu, R.K. Leak, A.K.F. Liou, S.F. Badylak, Z. Liu, J. Zhang, J. Chen, L. Chen, Implantation of brain-derived extracellular matrix enhances neurological recovery after traumatic brain injury, Cell Transplant. 26 (7) (2017) 1224–1234.

[16] N. Mukherjee, A. Adak, S. Ghosh, Recent trends in the development of peptide and protein-based hydrogel therapeutics for the healing of CNS injury, Soft Matter 16 (44) (2020) 10046–10064.

[17] M.F.P. Graca, S.P. Miguel, C.S.D. Cabral, I.J. Correia, Hyaluronic acid-based wound dressings: a review, Carbohydr. Polym. 241 (2020), 116364.

[18] H. Cortes, I.H. Caballero-Florán, N. Mendoza-Muñoz, E.N. Córdova-Villanueva, L. Escutia-Guadarrama, G. Figueroa-González, O.D. Reyes-Hernández, M. González-Del Carmen, M. Varela-Cardoso, J.J. Magaña, B. Florán, M.L. Del Prado-Audelo, G. Leyva-Gómez, Hyaluronic acid in wound dressings, Cell. Mol. Biol. (Noisy-Le-Grand) 66 (4) (2020) 191–198.

[19] K.C. Castro, M.G.N. Campos, L.H.I. Mei, Hyaluronic acid electrospinning: challenges, applications in wound dressings and new perspectives, Int. J. Biol. Macromol. 173 (2021) 251–266.

[20] S. Vasvani, P. Kulkarni, D. Rawtani, Hyaluronic acid: a review on its biology, aspects of drug delivery, route of administrations and a special emphasis on its approved marketed products and recent clinical studies, Int. J. Biol. Macromol. 151 (2020) 1012–1029.

[21] L. da Silva Meirelles, D. Simon, A. Regner, Neurotrauma: the crosstalk between neurotrophins and inflammation in the acutely injured brain, Int. J. Mol. Sci. 18 (5) (2017).

[22] S. Ciafrè, G. Ferraguti, P. Tirassa, A. Iannitelli, M. Ralli, A. Greco, G.N. Chaldakov, P. Rosso, E. Fico, M.P. Messina, V. Carito, L. Tarani, M. Ceccanti, M. Fiore, Nerve growth factor in the psychiatric brain, Riv. Psichiatr. 55 (1) (2020) 4–15.

[23] M.L. Rocco, M. Soligo, L. Manni, L. Aloe, Nerve growth factor: early studies and recent clinical trials, Curr. Neuropharmacol. 16 (10) (2018) 1455–1465.

[24] A. Alizadeh, L. Moradi, M. Katebi, J. Ai, M. Azami, B. Moradveisi, S.N. Ostad, Delivery of injectable thermo-sensitive hydrogel releasing nerve growth factor for

spinal cord regeneration in rat animal model, J. Tissue Viability 29 (4) (2020) 359–366.

[25] X. Hu, R. Li, Y. Wu, Y. Li, X. Zhong, G. Zhang, Y. Kang, S. Liu, L. Xie, J. Ye, J. Xiao, Thermosensitive heparin-poloxamer hydrogel encapsulated bFGF and NGF to treat spinal cord injury, J. Cell Mol. Med. 24 (14) (2020) 8166–8178.

[26] R. Li, Y. Li, Y. Wu, Y. Zhao, H. Chen, Y. Yuan, K. Xu, H. Zhang, Y. Lu, J. Wang, X. Li, X. Jia, J. Xiao, Heparin-poloxamer thermosensitive hydrogel loaded with bFGF and NGF enhances peripheral nerve regeneration in diabetic rats, Biomaterials 168 (2018) 24–37.

[27] S.H. Kim, S.H. Lee, J.E. Lee, S.J. Park, K. Kim, I.S. Kim, Y.S. Lee, N.S. Hwang, B.G. Kim, Tissue adhesive, rapid forming, and sprayable ECM hydrogel via recombinant tyrosinase crosslinking, Biomaterials 178 (2018) 401–412.

[28] R. Dimatteo, N.J. Darling, T. Segura, In situ forming injectable hydrogels for drug delivery and wound repair, Adv. Drug Deliv. Rev. 127 (2018) 167–184.

[29] L. Wang, J. Li, D. Zhang, S. Ma, J. Zhang, F. Gao, F. Guan, M. Yao, Dual-enzymatically crosslinked and injectable hyaluronic acid hydrogels for potential application in tissue engineering, RSC Adv. 10 (5) (2020) 2870–2876.

[30] J. Li, D. Zhang, S. Guo, C. Zhao, L. Wang, S. Ma, F. Guan, M. Yao, Dual-enzymatically cross-linked gelatin hydrogel promotes neural differentiation and neurotrophin secretion of bone marrow-derived mesenchymal stem cells for treatment of moderate traumatic brain injury, Int. J. Biol. Macromol. 187 (2021) 200–213.

[31] S. Schafer, H. Al-Qaddo, M. Gosau, R. Smeets, P. Hartjen, R.E. Friedrich, O.A. Nada, T. Vollkommer, A. Rashad, Cytocompatibility of bone substitute materials and membranes, In Vivo 35 (4) (2021) 2035–2040.

[32] Z. Li, A. Ramos, M.C. Li, Z. Li, S. Bhatta, A. Jeyaseelan, Y. Li, Q. Wu, S. Yao, J. Xu, Improvement of cell deposition by self-absorbent capability of freeze-dried 3D-bioprinted scaffolds derived from cellulose material-alginate hydrogels, Biomed. Phys. Eng. Express 6 (4) (2020), 045009.

[33] J. Balcucho, D.M. Narvaez, J.L. Castro-Mayorga, Antimicrobial and biocompatible polycaprolactone and copper oxide nanoparticle wound dressings against Methicillin-resistant Staphylococcus aureus, Nanomaterials 10 (9) (2020), 1692.

[34] J. Li, D. Zhang, S. Guo, C. Zhao, L. Wang, S. Ma, F. Guan, M. Yao, Dual-enzymatically cross-linked gelatin hydrogel promotes neural differentiation and neurotrophin secretion of bone marrow-derived mesenchymal stem cells for treatment of moderate traumatic brain injury, Int. J. Biol. Macromol. 187 (2021) 200–213.

[35] A.I.R. Maas, D.K. Menon, P.D. Adelson, N. Andelic, M.J. Bell, A. Belli, P. Bragge, A. Brazinova, A. Büki, R.M. Chesnut, G. Citerio, M. Coburn, D.J. Cooper, A.T. Crowder, E. Czeiter, M. Czosnyka, R. Diaz-Arrastia, J.P. Dreier, A.C. Duhaime, A. Ercole, T.A. van Essen, V.L. Feigin, G. Gao, J. Giacino, L.E. Gonzalez-Lara, R.L. Gruen, D. Gupta, J.A. Hartings, S. Hill, J.Y. Jiang, N. Ketharanathan, E.J.O. Kompanje, L. Lanyon, S. Laureys, F. Lecky, H. Levin, H.F. Lingsma, M. Maegele, M. Majdan, G. Manley, J. Marsteller, L. Mascia, C. McFadyen, S. Mondello, V. Newcombe, A. Palotie, P.M. Parizel, W. Peul, J. Piercy, S. Polinder, L. Puybasset, T.E. Rasmussen, R. Rossaint, P. Smielewski, J. Söderberg, S.J. Stanworth, M.B. Stein, N. von Steinbüchel, W. Stewart, E.W. Steyerberg, N. Stocchetti, A. Synnot, B. Te Ao, O. Tenovuo, A. Theadom, D. Tibboel, W. Videtta, K.K.W. Wang, W.H. Williams, L. Wilson, K. Yaffe, Traumatic brain injury: integrated approaches to improve prevention, clinical care, and research, Lancet Neurol. 16 (12) (2017) 987–1048.

[36] M. Galgano, G. Toshkezi, X. Qiu, T. Russell, L. Chin, L.R. Zhao, Traumatic brain injury: current treatment strategies and future endeavors, Cell Transplant. 26 (7) (2017) 1118–1130.

[37] D. Dougall, N. Poole, N. Agrawal, Pharmacotherapy for chronic cognitive impairment in traumatic brain injury, Cochrane Database Syst. Rev. 12 (2015), Cd009221.

[38] C.S. Cox Jr., Cellular therapy for traumatic neurological injury, Pediatr. Res. 83 (1–2) (2018) 325–332.

[39] S. Gennai, A. Monsel, Q. Hao, J. Liu, V. Gudapati, E.L. Barbier, J.W. Lee, Cell-based therapy for traumatic brain injury, Br. J. Anaesth. 115 (2) (2015) 203–212.

[40] Y. Zhou, A. Shao, W. Xu, H. Wu, Y. Deng, Advance of stem cell treatment for traumatic brain injury, Front. Cell. Neurosci. 13 (2019), 301.

[41] K. Zhang, Z. Shi, J. Zhou, Q. Xing, S. Ma, Q. Li, Y. Zhang, M. Yao, X. Wang, Q. Li, J. Li, F. Guan, Potential application of an injectable hydrogel scaffold loaded with mesenchymal stem cells for treating traumatic brain injury, J. Mater. Chem. B 6 (19) (2018) 2982–2992.

[42] W. Shi, C.J. Huang, X.D. Xu, G.H. Jin, R.Q. Huang, J.F. Huang, Y.N. Chen, S.Q. Ju, Y. Wang, Y.W. Shi, J.B. Qin, Y.Q. Zhang, Q.Q. Liu, X.B. Wang, X.H. Zhang, J. Chen, Transplantation of RADA16-BDNF peptide scaffold with human umbilical cord mesenchymal stem cells forced with CXCR4 and activated astrocytes for repair of traumatic brain injury, Acta Biomater. 45 (2016) 247–261.

[43] S. Liu, B. Sandner, T. Schackel, L. Nicholson, A. Chtarto, L. Tenenbaum, R. Puttagunta, R. Muller, N. Weidner, A. Blesch, Regulated viral BDNF delivery in combination with Schwann cells promotes axonal regeneration through capillary alginate hydrogels after spinal cord injury, Acta Biomater. 60 (2017) 167–180.

[44] C.C. Winter, K.S. Katiyar, N.S. Hernandez, Y.J. Song, L.A. Struzyna, J.P. Harris, D.K. Cullen, Transplantable living scaffolds comprised of micro-tissue engineered aligned astrocyte networks to facilitate central nervous system regeneration, Acta Biomater. 38 (2016) 44–58.

[45] R. Rauti, N. Renous, B.M. Maoz, Mimicking the brain extracellular matrix in vitro: a review of current methodologies and challenges, Isr. J. Chem. 60 (12) (2019) 1141–1151.

[46] M.A. Keen, Hyaluronic acid in dermatology, Skinmed 15 (6) (2017) 441–448.

[47] Z. Han, C.P. Wang, N. Cong, Y.Y. Gu, R. Ma, F.L. Chi, Therapeutic value of nerve growth factor in promoting neural stem cell survival and differentiation and protecting against neuronal hearing loss, Mol. Cell. Biochem. 428 (1–2) (2017) 149–159.

[48] S. Schwarz, A. Lehmbecker, W. Tongtako, K. Hahn, Y. Wang, F. Felmy, I. Zdora, G. Brogden, K. Branitzki-Heinemann, M. von Köckritz-Blickwede, W. Baumgärtner, I. Gerhauser, Neurotrophic effects of G(M1) ganglioside, NGF, and FGF2 on canine dorsal root ganglia neurons in vitro, Sci. Rep. 10 (1) (2020), 5380.

[49] Y. Zhang, D. An, Y. Pardo, A. Chiu, W. Song, Q. Liu, F. Zhou, S.P. McDonough, M. Ma, High-water-content and resilient PEG-containing hydrogels with low fibrotic response, Acta Biomater. 53 (2017) 100–108.

[50] L. Li, C. Lu, L. Wang, M. Chen, J. White, X. Hao, K.M. McLean, H. Chen, T.C. Hughes, Gelatin-based photocurable hydrogels for corneal wound repair, ACS Appl. Mater. Interfaces 10 (16) (2018) 13283–13292.

[51] K. Ravina, D.I. Briggs, S. Kislal, Z. Warraich, T. Nguyen, R.K. Lam, T.I. Zarembinski, M. Shamloo, Intracerebral delivery of brain-derived neurotrophic factor using HyStem®-C hydrogel implants improves functional recovery and reduces neuroinflammation in a rat model of ischemic stroke, Int. J. Mol. Sci. 19 (12) (2018).

[52] M. Zeeshan, M. Hamidi, T. O'Keeffe, E.H. Bae, K. Hanna, R.S. Friese, N. Kulvatunyou, E.R. Zakaria, L. Gries, A. Tang, B. Joseph, Propranolol attenuates cognitive, learning, and memory deficits in a murine model of traumatic brain injury, J. Trauma Acute Care Surg. 87 (5) (2019) 1140–1147.

[53] Y. Zhang, Y. Zhang, M. Chopp, Z.G. Zhang, A. Mahmood, Y. Xiong, Mesenchymal stem cell-derived exosomes improve functional recovery in rats after traumatic brain injury: a dose-response and therapeutic window study, Neurorehabilitation Neural Repair 34 (7) (2020) 616–626.

[54] E.A. van Vliet, X.E. Ndode-Ekane, L.J. Lehto, J.A. Gorter, P. Andrade, E. Aronica, O. Gröhn, A. Pitkänen, Long-lasting blood-brain barrier dysfunction and neuroinflammation after traumatic brain injury, Neurobiol. Dis. 145 (2020), 105080.

[55] L.B. Tucker, A.G. Velosky, J.T. McCabe, Applications of the Morris water maze in translational traumatic brain injury research, Neurosci. Biobehav. Rev. 88 (2018) 187–200.

[56] D.C. Morris, W.L. Cheung, R. Loi, T. Zhang, M. Lu, Z.G. Zhang, M. Chopp, Thymosin β4 for the treatment of acute stroke in aged rats, Neurosci. Lett. 659 (2017) 7–13.